Potential impact of Aeroclipper observations targeting tropical cyclone in the Western Pacific

Miki Hattori, Hugo Bellenger, Jean-philippe Duvel, Takeshi Enomoto

Received: 8 October 2023 | Revised: 19 February 2024 | Accepted: 15 March 2024

DOI: 10.1002/asl.1234

RESEARCH ARTICLE

Atmospheric Science Letters RMetS

Potential impact of Aeroclipper observations targeting tropical cyclone in the Western Pacific

Miki Hattori[1] | **Hugo Bellenger**[2] | **Jean-Philippe Duvel**[2] | **Takeshi Enomoto**[1,3]

[1]Japan Agency for Marine-Earth Science and Technology (JAMSTEC), Yokosuka, Kanagawa, Japan

[2]Laboratoire de Météorologie Dynamique, Paris, France

[3]Disaster Prevention Research Institute, Kyoto University, Uji, Kyoto, Japan

Correspondence
Miki Hattori, Japan Agency for Marine-Earth Science and Technology, 2–15 Natsushima-Cho, Yokosuka-city, Kanagawa 2370061, Japan.
Email: mhattori@jamstec.go.jp

Funding information
ANR, the French National Research Agency, Grant/Award Number: ANR-19-ASTR-0011; CNRS-IEA

Abstract

The Aeroclipper is a new balloon device that can be attracted and captured by tropical cyclones (TC) and perform continuous in situ measurements at the air–sea interfaces. To estimate the potential effect of Aeroclipper observations on the analysis of TCs, virtual Aeroclipper observations targeting TC Haima (October 2016) were synthesized using an idealized surface pressure distribution and best track data and were assimilated using an ensemble data assimilation system. Results show that the assimilation of Aeroclipper measurements may provide a more accurate representation of the TC pressure, wind, and temperature in analyses. This also leads to improved precipitation around the Philippines. The ensemble spread shows that the Aeroclipper measurement assimilation has an impact on the analyses that extends into the tropics from the early stages of TC development. These impact signals propagate westward with easterly waves and eastward with large-scale convective disturbances. Although the underlying mechanisms need to be further examined and tested using real Aeroclipper measurements, the present study shows that these balloons could provide valuable observations to improve the precision of analyses in presence of a TC. This is a first step toward a study of the impact of the Aeroclipper measurement on TC forecast.

KEYWORDS

Aeroclipper, ensemble data assimilation, virtual observation

1 | INTRODUCTION

In situ observations of tropical cyclones (TCs) are necessary to precisely monitor TC intensity in addition to estimates provided by satellite using method such as the Dvorak technique (Dvorak, 1984; Velden et al., 2006). TC intensity is proportional to the central pressure and is related to important characteristics of TCs such as convective activity and precipitation rate (e.g., Rao & MacArthur, 1994). Storm surge also depends on both TC intensity and displacement speed (Kohno et al., 2018). The forecast of TC intensity remains a considerable challenge (Ito, 2016; Rappaport et al., 2009; Yamaguchi et al., 2017), particularly for rapid intensifications (Ito, 2016). Moreover, the extent of TC-related disasters depends on the TC intensity itself.

The Dvorak technique is mainly based on empirical relationships between the evolution of the cloud patterns observed by satellite and the intensity of the TC (central pressure and maximum wind speed). However, the

empirical relationships on which it is based may be different from one basin to another and may evolve with climate change (Elsner et al., 2008; Mei & Xie, 2016; Webster et al., 2005). This technique has been poorly evaluated is some cyclonic basins (Indian Ocean and Western Pacific). Therefore, in situ observations remain essential for precise estimations of TC intensity (Holbach et al., 2023).

The Aeroclipper is a long-lasting (20–30 days) balloon drifting over the ocean following surface wind. The Aeroclipper balloon is held at ~30–50 m above the surface by a guiderope floating on the sea. It is designed to continuously measure the SST and air pressure, temperature, humidity, and wind speed at the balloon height with a time step of 1 min. During the validation of the Aeroclipper system under convective occurrences (VASCO) experiment in 2007 in the Indian Ocean (Duvel et al., 2009), two large Aeroclippers converged into TC Dora during the development stage and remained within the eye of the cyclone for the following days. Although no atmospheric data were transmitted due to a software issue, this event demonstrated the potential of Aeroclipper for TC monitoring. Evidently, continuous measurement of central position and central pressure of a TC allows a continuous estimate of its intensity and improve TC monitoring and potentially TC forecasts. Based on this assumption, a new light and affordable version of the Aeroclipper was developed by Laboratoire de Météorologie Dynamique since 2020. Aeroclipper measurements would be important in basins without airborne observations and have complementary advantages in basins covered by airborne measurements. For example, dropsondes deployed from aircraft are a powerful tool to monitor atmospheric vertical profiles at target points inside TCs. However, it incapable to obtain continuous observations of the TC intensity because of a limited flight time. Actual observations are not yet available to test the potential of Aeroclipper for TC forecast, because it is currently at a field-testing stage. This study is therefore based on virtual Aeroclipper measurements taken in simulated surface pressure time series.

Using these virtual measurements, a data assimilation experiment was conducted to evaluate the potential impact of Aeroclipper on the precision of the analysis and therefore on TC forecast. We used the Atmospheric General Circulation Model (AGCM) for Earth Simulator (AFES)-Local Ensemble Transform Kalman Filter (LETKF) data assimilation system (ALEDAS2; Enomoto et al., 2013; Miyoshi et al., 2007; Yamazaki et al., 2017) composed of the AGCM-AFES (Enomoto et al., 2008; Kuwano-Yoshida et al., 2010; Ohfuchi et al., 2004) and a LETKF (Hunt et al., 2007; Miyoshi & Yamane, 2007) with distance-based covariance localization. In ensemble data assimilation experiments, the analysis improvement may concern the ensemble mean or the ensemble spread. Even if the ensemble mean remains unchanged, a decrease in ensemble spread indicates that the analysis is more robust and should give a less dispersed ensemble forecasts. Changes in ensemble spread may concern only certain regions, and may also propagate from one region to another long after the observations have been assimilated. It has been used to assess the impact of observation campaigns in the Arctic (Inoue et al., 2009, 2013, 2015; Sato et al., 2017; Yamazaki et al., 2015), Antarctic (Sato et al., 2022), and the tropics (Hattori et al., 2016, 2017; Moteki et al., 2007, 2011) on the representation of surrounding atmospheric phenomena. Although this system has insufficient resolution to accurately represent the structure and intensity of TCs (e.g., Davis, 2018), it is suitable for evaluating the impact of Aeroclipper observations on global analysis. OSSE (observing system simulation experiment) is considered to be a highly effective method for evaluating nonexistent observational systems. In OSSE, the nature run refers to a high-resolution numerical simulation, which is considered to represent the true state and used to generate synthetic observations. As the low model resolution does not allow to generate synthetic Aeroclipper observations, we do not strictly speaking use an OSSE approach. Instead, we generate synthetic Aeroclipper sea level pressure (SLP) observations with higher resolution than our model and conduct impact assessments using ensemble data assimilation experiment. Our objective is to evaluate the potential of Aeroclippers to improve the precision of the meteorological analysis of the TC and of the surrounding regions. This is a first step toward a study of the impact of the Aeroclipper measurements assimilation on TC forecast.

2 | DATA AND METHODS

2.1 | Virtual Aeroclippers

Figure 1 shows the infrared brightness temperature image from the Multifunctional Transport Satellite (MTSAT-2) around TC Haima in its development stage at 00 UTC on 16 October 2016. Haima is typical of TCs forming in autumn in the Guam vicinity (a good site for Aeroclipper release) and landing in the northern part of the Philippines where they give large precipitation (Camargo et al., 2007; Kubota & Chan, 2009; Kubota & Wang, 2009). TC Haima was triggered as a tropical depression on 14 October ~700 km south of Guam. It subsequently moved to the west, intensified into a super-typhoon (TC category 5), and reached its maximum

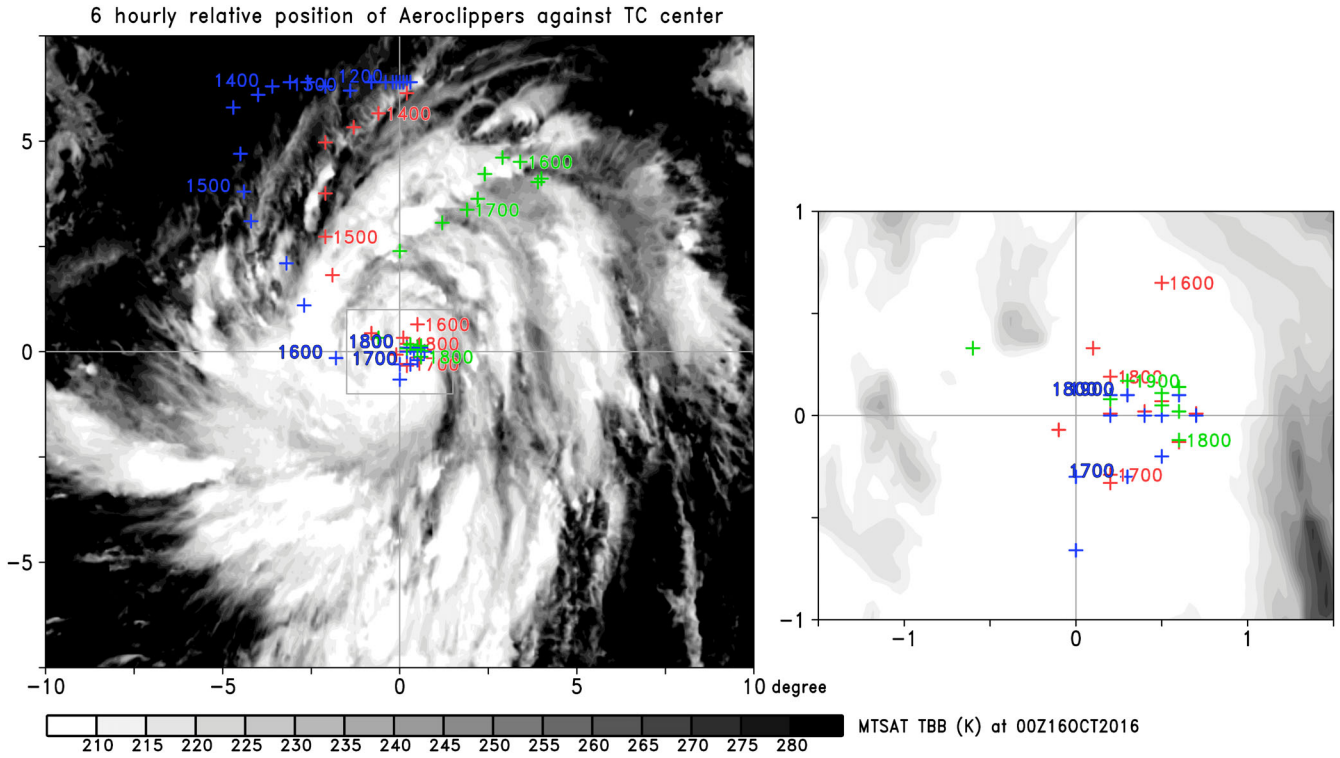

FIGURE 1 (Left) Successive positions of the three virtual Aeroclippers relative to the center of Haima at the corresponding time from 12 October at 00 GMT (noted 1200) to 19 October at 00 GMT (noted 1900). Aeroclipper #1 launched on 11 October from Guam (red), #2 launched on 13 October (blue), and #3 launched on 15 October (green). To illustrate the size of the tropical cyclones (TC), this is superimposed on the multifunctional transport satellite infrared image at 00 UTC on October 16, 2016 (Haima is then centered at 139.6° E 9.9° N). (Right) zoom on the TC center.

intensity shortly before landing on Luzon Island with a central pressure of 900 hPa on 19 October (Figure 2b).

Synthetic trajectories (Figure 1) and observations by three virtual Aeroclippers are computed using wind and pressure fields of ERA-Interim (ERA-I; Dee et al., 2011), which is a global atmospheric reanalysis with a 0.75° horizontal resolution produced by the European Centre for Medium-Range Weather Forecasts. Three virtual Aeroclippers are released from Guam on 11 (00 UTC), 13 (12 UTC), and 15 (12 UTC) October. Their quasi-Lagrangian trajectories are computed every 5 min using ERA-I zonal and meridional winds at 10 m linearly interpolated in time and space at the position of the Aeroclipper. The speed of the Aeroclipper (V_{AEC}) along this trajectory is estimated from an empirical relationship derived from previous experiments (Duvel et al., 2009), which relates V_{AEC} to the wind speed at 10 m (V_{10}).

$$V_{AEC} = 0.3\|V_{10}\|^{1.34}\frac{V_{10}}{\|V_{10}\|} \quad (1)$$

We subsequently applied a binomial smoothing filter (Marchand & Marmet, 1983) with a 12-h time window to avoid small-scale structures that are not useful given the low resolution of the mode. The trajectories of the virtual Aeroclippers (Figures 1 and 2a) shows that virtual Aeroclippers are successfully captured by TC Haima, and follow trochoidal trajectories, as observed for the two Aeroclippers captured in the TC Dora during the VASCO experiment.

Virtual Aeroclipper surface pressure observations (P_{AEC}) must be computed using a sharper radial pressure profile compared with what is given by ERA-I. Here, P_{AEC} is estimated based on (i) ERA-I SLP in the environment, (ii) the best track TC central pressure given by the Regional Specialized Meteorological Center (RSMC) Tokyo–Typhoon Center (Figure 2b), and (iii) a theoretical surface pressure function of ρ, the distance between the Aeroclipper and the center of the TC (Fujita, 1952; Ma et al., 2012), as follows:

$$P_{AEC}(\rho) = P_{env} + \frac{P_{BT} - P_{env}}{\sqrt{1 + \frac{1}{2}\left(\rho/\rho_{mp}\right)^2}} \quad (2)$$

where P_{env} is the environmental SLP at an "infinite" distance from the TC center and is set to be 1006 hPa by reference to the mean SLP from ERA-I in the region of the

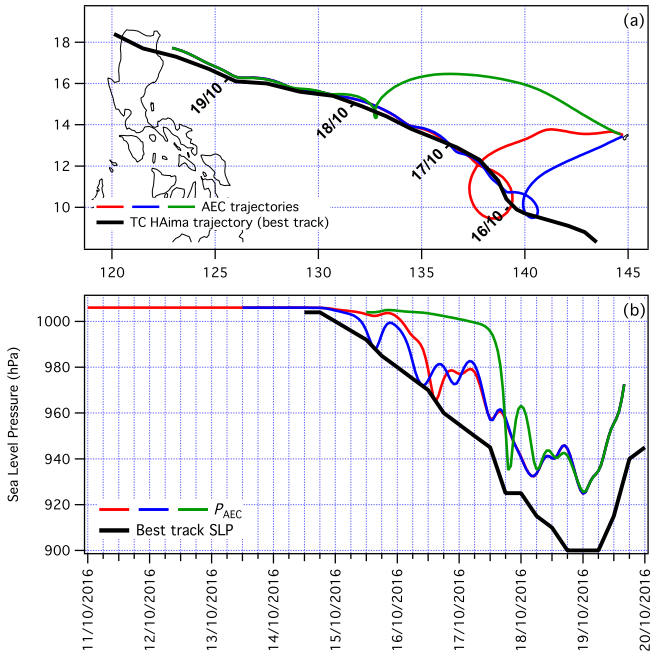

FIGURE 2 (a) Best track of TC Haima (thick black) and trajectories of the three virtual Aeroclippers that were used in the assimilation experiment (colored lines): Aeroclipper #1 (red), #2 (blue), and #3 (green). (b) Time series of: best track P_{BT} at TC Haima center (black) and P_{AEC} (colored lines) that is an estimate of the surface pressure measurement by the virtual Aeroclippers.

TC before it forms on 14 October, P_{BT} is the minimum SLP from the best track data, and ρ_{mp} is the radius of the maximum pressure gradient that can be approximated by half the maximum wind radius (Ma et al., 2012) taken from the best track data as the radius of 50-knot winds when they exist and 30-knot winds otherwise.

2.2 | The data assimilation experiment

An assimilation experiment for the virtual Aeroclipper observations was performed using ALEDAS2 with a resolution of T119 (triangular truncation with truncation wavenumber of 119, $1 \times 1^\circ$) in the horizontal direction and 48 levels (σ-level, up to ~3 hPa) in the vertical direction. A total of 63 ensemble members were calculated with a localization length of 400 km in the horizontal direction and 0.4 $\ln(p)$ for the log pressure coordinates in the vertical direction. The data assimilation window was 6 h. Asynchronous observations can be treated appropriately owing to the four-dimensional extension of the LETKF (Miyoshi & Yamane, 2007). There were seven 1-h time slots (±3 h from analysis time t) at each analysis; thus, observations were assimilated every hour. Observational data were prepared every 6 h from the National Centers for Environmental Prediction PREPBUFR (prepared binary universal form for the representation of meteorological data). The data included conventional atmospheric observations (upper air soundings, aircraft reports, wind profilers, surface land, and marine reports) and satellite-derived wind reports. Using ALEDAS2, the AFES-LETKF experimental ensemble reanalysis version 2 (ALERA2) data set from January 1, 2008 to January 4, 2021, which assimilates only PREPBUFR is produced.

In this study, to assess the impact of the virtual Aeroclipper SLP observations, we regard the 6-h ALERA2 data as the control run (CTL). CTL will be compared with an AEC experiment, which assimilates the SLP from the three virtual Aeroclippers (P_{AEC}), in addition to PREPBUFR. The experimental period was from October 10, 2016 to October 25, 2016. Although the virtual Aeroclipper observations must be stopped just before the first Aeroclipper reached Luzon on 20 October, the analysis process without the virtual Aeroclipper data ran continuously until 25 October.

According to the quality control (QC) procedure of ALEDAS2, observational data are assimilated when they do not significantly differ from the first guess of the model using a parameter-dependent gross error threshold. However, in this study, the gross error check procedure was not applied to the P_{AEC} in order to prevent it from rejecting Aeroclipper observations.

The risks due to the assimilation of a single P_{BT} value at the center of the TC have been indicated in previous studies (Chen & Snyder, 2007; Kunii, 2014). However, in this study, continuous measurements P_{AEC} along the Aeroclipper trajectory provides more widespread information during the convergence phase as well as after the capture in the TC eye (Figure 1). In addition, simultaneous observations using three Aeroclippers enables them to provide two-dimensional TC information before all three are captured. Thus, we consider this approach to be different from the one that directly use $P_{AEC} = P_{BT}$ (Heming, 2016), especially during the convergence phase when the assimilation of Aeroclipper observations indeed provides pressure and wind information in the surroundings, and possibly far from the TC center. After capture, the pressure measurement is closer to P_{BT}.

2.3 | Other data

The representation of the precipitation in the model is tested using the hourly rain rate with a $0.1 \times 0.1^\circ$ resolution provided by the global satellite mapping of precipitation (GSMaP, Kubota et al., 2020). To facilitate comparison, the GSMaP precipitation is first projected onto the AFES $1^\circ \times 1^\circ$ horizontal grid.

3 | RESULTS

3.1 | Virtual Aeroclippers

The three virtual Aeroclippers are launched from Guam Island ~4 days before, 1 day before, and 1 day after the initiation of the Haima depression (14 October) (Figure 2b). The first two Aeroclippers converged into the TC eye soon after triggering (16 and 17 October); whereas, the latter converged later when TC Haima approached the Philippines (Figure 2a). On October 20, Haima's eye crosses the Philippines, and the three virtual Aeroclippers are supposed to be destroyed as real Aeroclippers should be (because of the guiderope, the Aeroclipper only works over the Ocean). No Aeroclipper measurements are taken after October 20. After this date, only the remnant effect of the Aeroclippers is therefore influencing the ensemble analysis. The estimated value of P_{AEC} is ~20 hPa higher than the P_{BT} at the time of maximum Haima intensity (19 October; Figure 2b). The colored crosses in Figure 1 indicate the relative positions of the three Aeroclippers relative to the center of TC Haima. One can consider that there are multiple Aeroclipper observations until the last Aeroclipper converged into the TC eye on 18 October. This implies that our experiment is an assimilation of multiple Aeroclipper observations, including the values in the TC surroundings. As noted above, this is different from the assimilation of a single-point value at the center of the TC.

3.2 | TC intensity

Figure 3 shows the time series of the minimum SLP in TC Haima for the best track (P_{BT}) and for the ensemble average of AEC and CTL experiments. As expected, the assimilation procedure of the AEC experiment smooths out the virtual Aeroclipper measurements. It gives a minimum SLP of ~960 hPa (Figure 3) that is 40 hPa higher compared with P_{AEC} (Figure 2b) and 60 hPa higher compared with P_{BT} at time of maximum intensity of Haima. However, the assimilation of P_{AEC} gives an improvement of ~30 hPa compared with the CTL experiment that gives a minimum SLP of ~990 hPa. The differences between the two ensembles became discernible, as the first Aeroclipper converged into the depression on 16 October when P_{AEC} was below 980 hPa (Figure 2b). After this date, P_{AEC} and the minimum SLP in the AEC ensemble analysis both decreased progressively until 19 October, as for the Best Track SLP. After October 20, no Aeroclipper measurements are assimilated, and the minimum SLP difference between CTL and AEC is small.

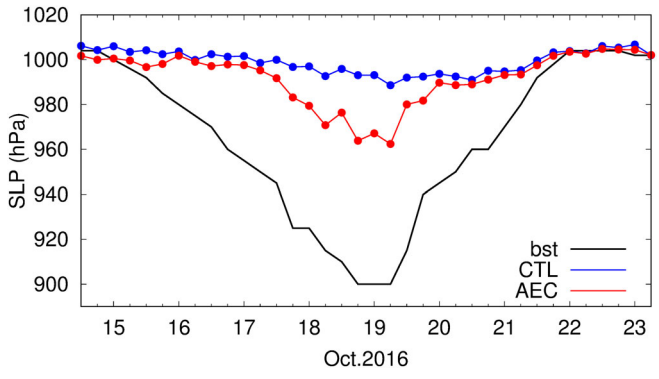

FIGURE 3 Time series of the ensemble-mean minimum SLP for Aeroclipper analysis (red) and CTL analysis (blue) and the minimum SLP from the best track (black). AEC, Aeroclipper.

3.3 | TC structure

The assimilation of P_{AEC} also improves the 3D structure of the modeled TC Haima. Figure 4 shows map of SLP and 925 hPa wind field, and the vertical cross-sections of wind speed and temperature anomalies in the CTL and AEC ensembles at the time of minimum SLP in Haima. In the AEC experiment, the surface wind pattern is more realistic with an eye apparently surrounded with larger wind with a smaller radius of maximum wind. The asymmetry of the wind field is also better represented with stronger wind on the right side relative to the direction of travel; a feature that is well-known (e.g., Gray, 1968; Hughes, 1952); however, this was not represented in the CTL. The assimilation of P_{AEC} strongly increases Haima's cyclonic circulation, with the 925 hPa wind peaking at ~50 m s^{-1} in the AEC analysis (Figure 4b) compared with ~30 m s^{-1} in the CTL analysis (Figure 4a). The steeper decrease in SLP within 2.5° from the TC center (Figure 4c) corresponds to a wind speed increase in AEC compared with CTL, which can be seen up to 400 hPa and peaks at 900 hPa (Figure 4d–f). The warm core structure in the eye is more developed in AEC analysis although its height is less than that of a typical TC warm core, with a maximum perturbation of +7°C at 800 hPa (Figure 4e).

3.4 | TC precipitation around the Philippines

TCs regularly generate extreme rainfall in the Philippines. For instance, Pfahl and Wernli (2012) found that ~50%–60% of extreme rainfall events in the Philippines are associated with TC occurrence. Figure 4 shows the hourly mean of 6-h forecast precipitation at 12 UTC on 19 October just before TC Haima landed on Luzon for the CTL and

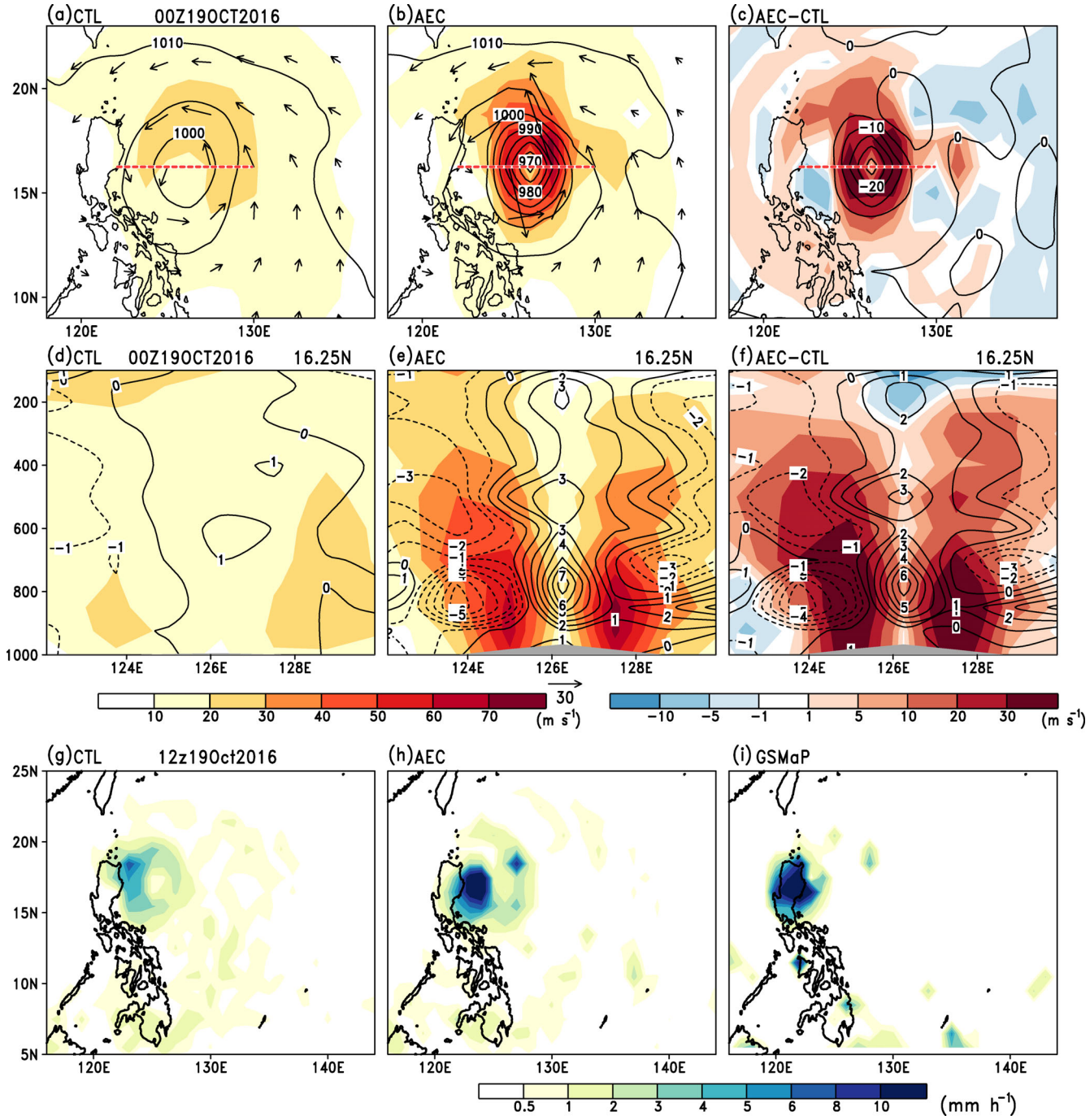

FIGURE 4 (a–c) Wind speed (color scale) and wind vector (arrow) at 925 hPa and SLP (contour) at 00 UTC on October 19, 2016, for (a) CTL analyses, (b) AEC analyses, and (c) AEC-CTL. (d–f) Vertical cross-section of wind speed (color scale) and temperature anomaly from the latitudinal average between 5° N and 25° N (black contour) at 00 UTC on October 19, 2016, for (d) CTL, (e) AEC, and (f) AEC-CTL. The contour interval of the solid and dashed black lines is 1°. Hourly means of 6-h forecast precipitation (mm h^{-1}) at 12 UTC on October 19, 2016, for (g) CTL, (h) AEC, and (i) observed precipitation by GSMaP.

AEC ensembles. At that time, GSMaP gives maximum rainfall rate larger than 10 mm h^{-1} over land (Figure 4i) while CTL gives <6 mm h^{-1} with almost no rain over the land (Figure 4g) and AEC gives more than 10 mm h^{-1} over the ocean to the east of Luzon with increase to 6 mm h^{-1} over the land (Figure 4h).

3.5 | Impact on the tropics and the mid-latitudes

As a characteristic of ensemble data assimilation, impact of the observational data assimilation can be evaluated by how much the ensemble spread changes, even if the

ensemble mean has no clear differences (Hattori et al., 2016, 2017; Moteki et al., 2007, 2011). In the present study, an index of analysis ensemble spread reduction rate (SRR) in AEC is defined as:

$$\mathrm{SRR} = \frac{\mathrm{spread}_{\mathrm{CTL}} - \mathrm{spread}_{\mathrm{AEC}}}{\mathrm{spread}_{\mathrm{CTL}}} \times \frac{K_s}{K} \times 100. \qquad (3)$$

where $\mathrm{spread}_{\mathrm{CTL}}$ and $\mathrm{spread}_{\mathrm{AEC}}$ are the average spread on the grid points considered. To remove meaningless noise in the spread difference, SRR is calculated considering only the ensemble of grid points with significant differences in the spreads, averaged spatial and/or temporal, and weighted for the locations that include more significant grid points. K represents the total number of grid points in a target domain (e.g., grid number in averaged vertical levels × number of time steps used to create the average). K_s represents the number of grid points at which the significant spread differences are extracted using a statistical significance test. A locally positive SRR means that the AEC ensemble spread is reduced and therefore that the analysis is more robust for this region. The SRR value indicates the local magnitude of the improvement. SRR is a useful but qualitative assessment. In some cases, an analysis that captures more realistic and detailed structures of a phenomenon may even lead to a negative SRR (this is the case near a TC). Therefore, a locally negative SRR does not mean that the average analysis is worse (i.e., further from the true atmospheric state), it means that the forecasts are likely to be more dispersed nearby. Conversely, a positive SRR over a large area indicates that the analysis is more robust for that area and will potentially lead to a less dispersed ensemble forecast. Figure 5a shows SRR of the meridional wind between 1000 and 100 hPa averaged from October 11, 2016 to October 25, 2016. This diagnostic

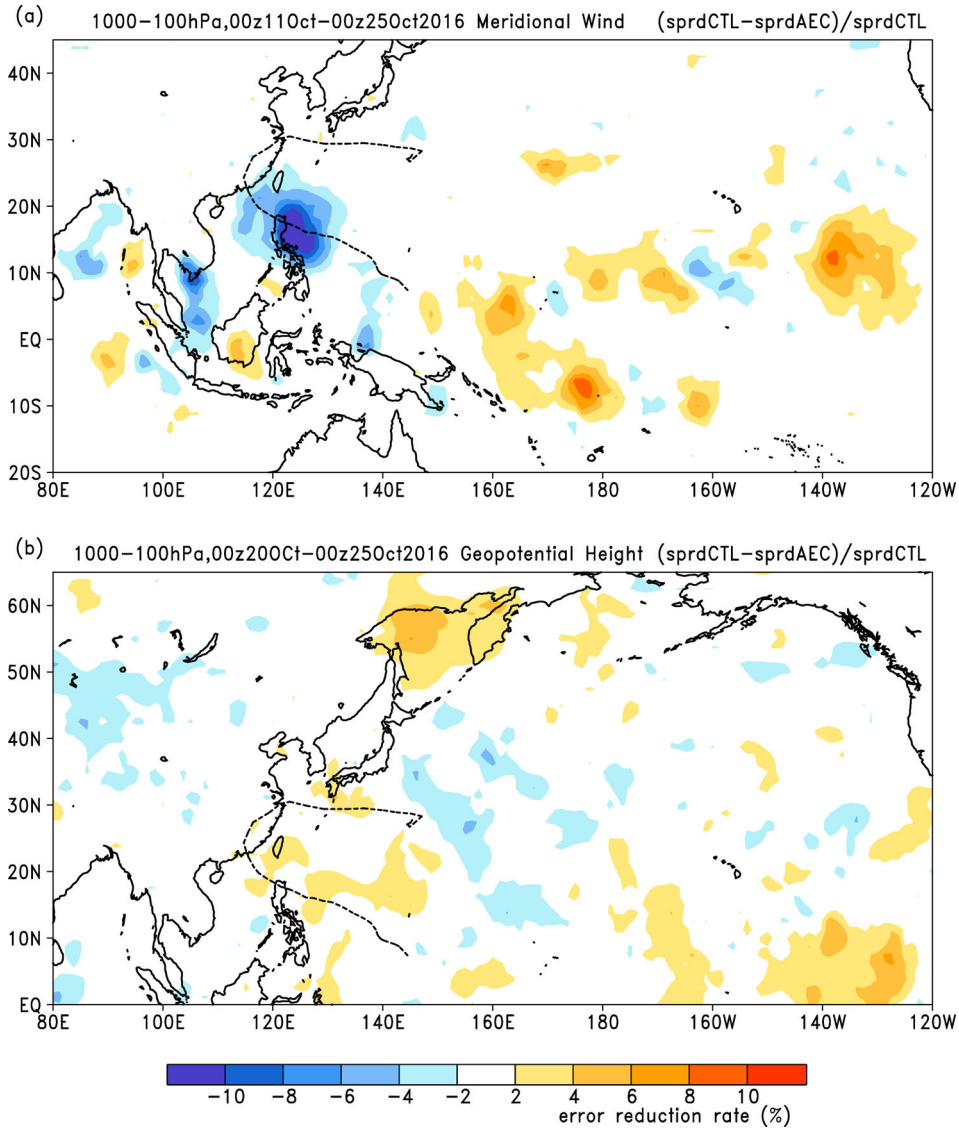

FIGURE 5 (a) Analysis ensemble SRR of meridional wind averaged between 1000 and 100 hPa and from October 11, 2016 to October 25, 2016. (b) As in (a), but for geopotential height averaged from October 20, 2016 to October 25, 2016. The black dashed line indicates the best track of tropical cyclones Haima.

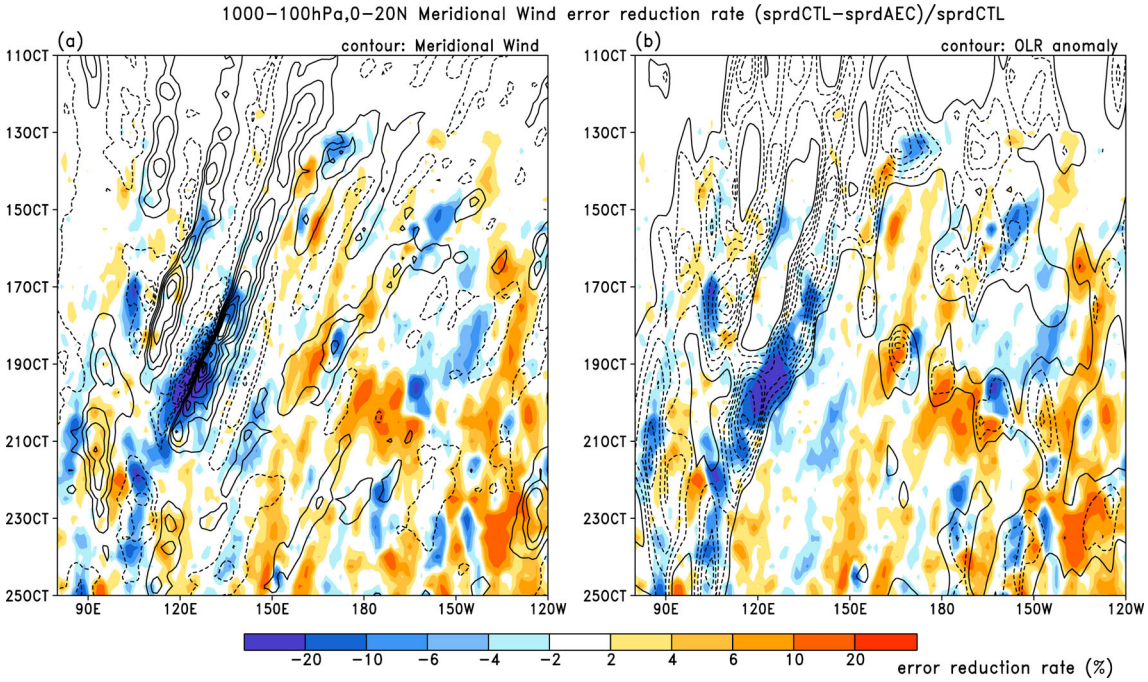

FIGURE 6 (a) Time-longitude diagrams of analysis ensemble SRR of the meridional wind averaged between 1000 and 100 hPa (color scale) and meridional wind speed at 850 hPa (contours) averaged from 0° N to 20° N from October 11, 2016 to October 25, 2016. (b) As in (a), but the contours are the OLR anomaly relative to the seasonal mean from September 1 to November 30.

indicates that the effects of data assimilation propagated far into the tropics throughout the experimental period from the early stage of TC development. Hovmöller diagrams of SRR (Figure 6) show positive (orange) and negative (blue) impact signals propagating westward with easterly waves represented by repeating patterns of positive and negative meridional winds (contour in Figure 6a). Moreover, impact signals propagate eastward at a slower speed, accompanied by large-scale convective disturbances represented by negative outgoing longwave radiation (OLR) anomalies (contour in Figure 6b). The large negative SRR around 120E indicates the increased analysis uncertainty due to the assimilation of the virtual Aeroclipper measurements in the strong gradients generated by TC Haima.

Figure 5b shows the analysis ensemble SRR of the geopotential height between 1000 and 100 hPa averaged from October 20, 2016 to October 25, 2016. A large positive impact signal appeared over the Okhotsk Sea.

4 | DISCUSSION AND CONCLUSION

This study presents a preliminary assessment of the potential improvements of meteorological analysis due to the assimilation of surface pressure data from continuous Aeroclipper measurements in the surrounding and in the eye of a TC. Virtual Aeroclippers are used here to mimic real measurements during the converging stage, and thus relatively far from the center, and after the balloon capture in the eye where Aeroclipper measure a surface pressure close to the minimum. In order to have a more statistical approach of these two measurement types, three Aeroclippers are used that gives distributed information of SLP in and around the TC at different stage of TC Haima.

Results shows that the assimilation of surface pressure from virtual Aeroclippers measurements improved the meteorological analysis of TC intensity. This increased intensity is associated with an improvement in the representation of the vertical structure of the TC, with in particular the formation of a warm core in the eye. Rainfall associated with TC Haima over Luzon Island in the Philippines also increased when the Aeroclipper measurements are assimilated. Using the index of analysis ensemble SRR, it is indicated that the statistically significant impact of the Aeroclipper observations propagates in the tropics and in mid-latitudes. Results suggest that for the particular situation studied here, the impact signal propagations are related to the easterly waves and large-scale convective disturbances in the tropics.

Due to (i) the relatively coarse horizontal resolution ($1 \times 1°$) of the model, (ii) to the use of ERA-I to estimate the trajectory of the Aeroclippers, and (iii) to the use a

theoretical relation to estimate the Aeroclipper measurements, this assessment should be considered as preliminary. Also, at this experimental stage, the QC of the difference between the observations and the first guess was turned off in ALEDAS2 to allow the Aeroclipper surface pressure data to be considered. In actual observations, it should be noted that a QC process is required to avoid inappropriate data assimilation while considering the large differences between the model and observed TC values. This QC procedure will then have to be adapted to allow the assimilation of Aeroclipper measurements near a TC center.

AUTHOR CONTRIBUTIONS

Miki Hattori: Conceptualization; data curation; formal analysis; investigation; visualization; writing – original draft. **Hugo Bellenger:** Conceptualization; data curation; formal analysis; methodology; visualization; writing – review and editing. **Jean-Philippe Duvel:** Funding acquisition; methodology; project administration; supervision; writing – review and editing. **Takeshi Enomoto:** Supervision; writing – review and editing.

ACKNOWLEDGMENTS

We are grateful to the RSMC Tokyo–Typhoon Center for providing the TC best track data. We would also like to thank the Earth Observation Research Center, Japan Aerospace Exploration Agency for the distribution of GSMaP products, and the Center for Environmental Remote Sensing Chiba University (CEReS) for archiving and distributing gridded data from MTSAT-2 (https://ceres.chiba-u.jp/database-ceres/satellite/). This work was supported by ANR, the French National Research Agency (ANR-19-ASTR-0011), and the CNRS-IEA. The Earth Simulator was used with the support of JAMSTEC.

CONFLICT OF INTEREST STATEMENT

The authors report no conflict of interest.

DATA AVAILABILITY STATEMENT

The data produced the findings of this study are available from the corresponding author upon reasonable request.

ORCID

Miki Hattori https://orcid.org/0000-0003-1444-3809

REFERENCES

Camargo, S.J., Robertson, A.W., Gaffney, S.J., Smyth, P. & Ghil, M. (2007) Cluster analysis of typhoon tracks. Part I: general properties. *Journal of Climate*, 20, 3635–3653.

Chen, Y. & Snyder, C. (2007) Assimilating vortex position with an ensemble Kalman filter. *Monthly Weather Review*, 135, 1828–1845.

Davis, C.A. (2018) Resolving tropical cyclone intensity in models. *Geophysical Research Letters*, 45, 2082–2087.

Dee, D.P., Uppala, S.M., Simmons, A.J., Berrisford, P., Poli, P., Kobayashi, S. et al. (2011) The ERA-interim reanalysis: configuration and performance of the data assimilation system. *Quarterly Journal of the Royal Meteorological Society*, 137, 553–597. Available from: https://doi.org/10.1002/qj.828

Duvel, J.-P., Basdevant, C., Bellenger, H., Reverdin, G., Vargas, A. & Vialard, J. (2009) The Aeroclipper–a new device to explore convective systems and cyclones. *Bulletin of the American Meteorological Society*, 90, 63–71.

Dvorak, V.F. (1984) Tropical cyclone intensity analysis using satellite data. *NOAA Technical Report*, 11, 45.

Elsner, J.B., Kossin, J.P. & Jagger, T.H. (2008) The increasing intensity of the strongest tropical cyclones. *Nature*, 455, 92–95.

Enomoto, T., Kuwano-Yoshida, A., Komori, N. & Ofuchi, W. (2008) Description of AFES 2: improvements for high-reso- lution and coupled simulations. In: Hamilton, K. & Ohfuchi, W. (Eds.) *High resolution numerical modelling of the atmosphere and ocean*. New York: Springer, pp. 77–97.

Enomoto, T., Miyoshi, T., Moteki, Q., Inoue, J., Hattori, M., Kuwano-Yoshida, A. et al. (2013) Observing-system research and ensemble data assimilation at JAMSTEC. In: Park, S.K. & Xu, L. (Eds.) *Data assimilation for atmospheric, oceanic and hydrologic applications*, Vol. II. Berlin, Heidelberg: Springer, pp. 509–526.

Fujita, T. (1952) Pressure distribution within a typhoon. *Geophysical Magazine*, 23, 437–451.

Gray, W.M. (1968) On the balance of forces and radial accelerations in hurricanes. *Quarterly Journal Royal Meteorological Society*, 88, 430–458.

Hattori, M., Matsumoto, J., Ogino, S.-Y., Enomoto, T. & Miyoshi, T. (2016) The impact of additional radiosonde observations on the analysis of disturbances in the South China Sea during VPREX2010. *Scientific Online Letters on the Atmosphere*, 12, 75–79. Available from: https://doi.org/10.2151/sola.2016-018

Hattori, M., Yamazaki, A., Ogino, S.-Y., Peiming, W. & Matsumoto, J. (2017) Impact of the radiosonde observations of cold surge over the Philippine Sea on the tropical region and the southern hemisphere in December 2012. *Scientific Online Letters on the Atmosphere*, 13, 19–24. Available from: https://doi.org/10.2151/sola.2017-004

Heming, J.T. (2016) Met Office unified model tropical cyclone performance following major changes to the initialization scheme and a model upgrade. *Weather and Forecasting*, 31, 1433–1449.

Holbach, H.M., Bousquet, O., Bucci, L., Chang, P., Cione, J., Ditchek, S. et al. (2023) Recent advancements in aircraft and in situ observations of tropical cyclones. *Tropical Cyclone Research and Review*, 12, 81–99. Available from: https://doi.org/10.1016/j.tcrr.2023.06.001

Hughes, L.A. (1952) On the low-level wind structure of tropical storms. *Journal of Meteorology*, 5, 422–428.

Hunt, B.R., Kostelich, E.J. & Szunyogh, I. (2007) Efficient data assimilation for spatiotemporal chaos: a local ensemble transform Kalman filter. *Physica D*, 230, 112–126.

Inoue, J., Enomoto, T. & Hori, M.E. (2013) The impact of radiosonde data over the ice-free Arctic Ocean on the atmospheric circulation in the northern hemisphere. *Geophysical Research Letters*, 40, 864–869. Available from: https://doi.org/10.1002/grl.50207

Inoue, J., Enomoto, T., Miyoshi, T. & Yamane, S. (2009) Impact of observations from Arctic drifting buoys on the reanalysis of surface fields. *Geophysical Research Letters*, 36, L08501.

Inoue, J., Yamazaki, A., Ono, J., Dethloff, K., Maturilli, M., Neuber, R. et al. (2015) Additional Arctic observations improve weather and sea-ice forecasts for the Northern Sea route. *Scientific Reports*, 5, 16868. Available from: https://doi.org/10.1038/srep16868

Ito, K. (2016) Errors in tropical cyclone intensity forecast by RSMC Tokyo and statistical correction using environmental parameters. *Scientific Online Letters on the Atmosphere*, 12, 247–252. Available from: https://doi.org/10.2151/sola.2016-049

Kohno, N., Dube, S.K., Entel, M., Fakhruddin, S.H.M., Greenslade, D., Leroux, M.D. et al. (2018) Recent progress in storm surge forecasting. *Tropical Cyclone Research and Review*, 7(2), 128–139. Available from: https://doi.org/10.6057/2018TCRR02.04

Kubota, H. & Chan, J.C.L. (2009) Interdecadal variability of tropical cyclone landfall in The Philippines from 1902 to 2005. *Geophysical Research Letters*, 36, L12802.

Kubota, H. & Wang, B. (2009) How much do tropical cyclones affect seasonal and interannual rainfall variability over the western North Pacific? *Journal of Climate*, 22, 5495–5510.

Kubota, T., Aonashi, K., Ushio, T., Shige, S., Takayabu, Y.N., Kachi, M. et al. (2020) *Global satellite mapping of precipitation (GSMaP) products in the GPM era, satellite precipitation measurement. Advances in global change research*, Vol. 67. Cham: Springer.

Kunii, M. (2014) Data assimilation experiments for tropical cyclones with the NHM-LETKF. *CAS/JSC WGNE Research activities in atmospheric and oceanic modeling*, 44, 1.09–1.10.

Kuwano-Yoshida, A., Enomoto, T. & Ohfuchi, W. (2010) An improved PDF cloud scheme for climate simula- tions. *Quarterly Journal of the Royal Meteorological Society*, 136, 1583–1597.

Ma, Y., Kafatos, M. & Davidson, N.E. (2012) Surface pressure profiles, vortex structure and initialization for hurricane prediction. Part I: analysis of observed and synthetic structures. *Meteorology and Atmospheric Physics*, 117, 5–23. Available from: https://doi.org/10.1007/s00703-012-0190-z

Marchand, P. & Marmet, L. (1983) Binomial smoothing filter: a way to avoid some pitfalls of least-squares polynomial smoothing. *Revues of Scientific Instrumentation*, 54(8), 1034–1041.

Mei, W. & Xie, S.-P. (2016) Intensification of lanfalling typhoons over the northwest Pacific since the late 1970s. *Nature Geoscience*, 9, 753–757. Available from: https://doi.org/10.1038/NGEO2792

Miyoshi, T. & Yamane, S. (2007) Local ensemble transform Kalman filtering with an AGCM at a T159/L48 resolution. *Monthly Weather Review*, 135, 3841–3861.

Miyoshi, T., Yamane, S. & Enomoto, T. (2007) Localizing the error covariance by physical distances within a local ensemble transform Kalman filter (LETKF). *Scientific Online Letters on the Atmosphere*, 3, 89–92. Available from: https://doi.org/10.2151/sola.2007-023

Moteki, Q., Shirooka, R., Yoneyama, K., Geng, B., Katsumata, M., Ushiyama, T. et al. (2007) The impact of the assimilation of dropsonde observations during PALAU2005 in ALERA. *Scientific Online Letters on the Atmosphere*, 3, 97–100.

Moteki, Q., Yoneyama, K., Shirooka, R., Kubota, H., Yasunaga, K., Suzuki, J. et al. (2011) The influence of observations propagated by convectively coupled equatorial waves. *Quarterly Journal of the Royal Meteorological Society*, 137, 641–655.

Ohfuchi, W., Nakamura, H., Yoshioka, M.K., Enomoto, T., Takaya, K., Peng, X. et al. (2004) 10-km mesh meso-scale resolving simulations of the global atmosphere on the earth simulator: preliminary outcomes of AFES (AGCM for the earth simulator). *Journal of the Earth Simulator*, 1, 8–34.

Pfahl, S. & Wernli, H. (2012) Quantifying the relevance of cyclones for precipitation extremes. *Journal of Climate*, 25, 6770–6780.

Rao, G.V. & MacArthur, P.D. (1994) The SSM/I estimated rainfall amounts of tropical cyclones and their potential in predicting the cyclone intensity changes. *Monthly Weather Review*, 122, 1568–1574.

Rappaport, E.N., Franklin, J.L., Avila, L.A., Baig, S.R., Beven, J.L., Blake, E.S. et al. (2009) Advances and challenges at the National Hurricane Center. *Weather and Forecasting*, 24, 395–419. Available from: https://doi.org/10.1175/2008WAF2222128.1

Sato, K., Inoue, J., Yamazaki, A., Kim, J.-H., Maturilli, M., Dethloff, K. et al. (2017) Improved forecasts of winter weather extremes over midlatitudes with extra Arctic observations. *Journal of Geophysical Research, Oceans*, 122, 775–787. Available from: https://doi.org/10.1002/2016JC012197

Sato, K., Inoue, J., Yamazaki, A., Tomikawa, Y. & Sato, K. (2022) Reduced error and uncertainty in analysis and forecasting in the southern hemisphere through assimilation of PANSY radar observations from Syowa Station: a midlatitude extreme cyclone case. *Quarterly Journal of the Royal Meteorological Society*, 148, 3115–3130. Available from: https://doi.org/10.1002/qj.4347

Velden, C., Harper, B., Wells, F., Beven, J.L., Zehr, R., Olander, T. et al. (2006) The Dvorak tropical cyclone intensity estimation technique: a satellite-based method that has endured for over 30 years. *Bulletin of the American Meteorological Society*, 87, 1195–1210.

Webster, P.J., Holland, G.J., Curry, J.A. & Chang, H.-R. (2005) Changes in tropical cyclone number, duration, and intensity in a warming environment. *Science*, 309, 1844–1846.

Yamaguchi, M., Ishida, J., Sato, H. & Nakagawa, M. (2017) WGNE Intercomparison of tropical cyclone forecasts by operational global models: a quarter-century and beyond. *Bulletin of the American Meteorological Society*, 98, 2337–2349.

Yamazaki, A., Enomoto, T., Miyoshi, T., Kuwano-Yoshida, A. & Komori, N. (2017) Using observations near the poles in the AFES-LETKF data assimilation system. *Scientific Online Letters on the Atmosphere*, 13, 41–46. Available from: https://doi.org/10.2151/sola.2017-008

Yamazaki, A., Inoue, J., Dethloff, K., Maturilli, M. & König-Langlo, G. (2015) Impact of radiosonde observations on forecasting summertime Arctic cyclone formation. *Journal of Geophysical Research*, 120, 3249–3273.

How to cite this article: Hattori, M., Bellenger, H., Duvel, J.-P., & Enomoto, T. (2024). Potential impact of Aeroclipper observations targeting tropical cyclone in the Western Pacific. *Atmospheric Science Letters*, e1234. https://doi.org/10.1002/asl.1234